The Stability of Gold Iodides in the Gas Phase and the Solid State

Tilo Söhnel,[a] Reuben Brown,[a] Lars Kloo,[b] and Peter Schwerdtfeger*[a]

Abstract: The stability of gold iodides in the oxidation state +I and +III is investigated at the ab initio and density functional level using relativistic and nonrelativistic energy-adjusted pseudopotentials for gold and iodine. The calculations reveal that relativistic effects stabilize the higher oxidation state of gold as expected, that is Au_2I_6 is thermodynamically stable at the relativistic level, whilst at the nonrelativistic level the complex of two iodine molecules weakly bound to both gold atoms in Au_2I_2 is energetically preferred. The rather low stability of AuI_3 with respect to dissociation into AuI and I_2 will make it difficult to isolate this species in the solid state as (possibly) Au_2I_6 or detect it by matrix-isolation techniques. The monomer AuI_3 is Jahn–Teller distorted from the ideal trigonal planar (D_{3h}) form, but adopts a Y-shaped structure (in contrast to AuF_3 and $AuCl_3$), and in the nonrelativistic case can be described as I_2 weakly bound to AuI. Relativistic effects turn AuI_3 from a static Jahn–Teller system to a dynamic one. For the yet undetected gas-phase species AuI accurate coupled-cluster calculations for the potential energy curve are used to predict vibrational–rotational constants. Solid-state density functional calculations are performed for AuI and Au_2I_6 in order to predict cohesive energies.

Keywords: gold · iodine · Jahn–Teller distortion · relativistic effects · solid-state structures

Introduction

Gold(I) iodides are well known as solid-state compounds. AuI adopts a polymeric zigzag structure with linear I-Au-I units similar to AuCl and AuBr.[1, 2] AuI has not been detected yet in the gas phase or by matrix isolation; however, Evans and Gerry have quite recently carried out microwave studies of AuF, AuCl, and AuBr.[3] The linear gold(I) complex $[AuI_2]^-$ is also known in the solid state and is very stable in aqueous solution. Unlike $AuBr_2^-$ and $AuCl_2^-$, AuI_2^- does not disproportionate (in this case to AuI_4^- and metallic gold). Thus, the question of the stability of gold iodides in the higher oxidation state +3 remains open. Only a few compounds with AuI_4^- units are known and they are of rather limited stability.[4, 5] In aqueous solution AuI_4^- lies in equilibrium with AuI_2^-, that is $AuI_4^- \rightleftharpoons AuI_2^- + I_2$.[6] $AuF_3(s)$, $Au_2Cl_6(s)$, and $Au_2Br_6(s)$ are all known, whilst $Au_2I_6(s,g)$ has not been prepared yet.[1]

The monomers AuF_3 and $AuCl_3$ undergo a first-order Jahn–Teller distortion along the E' mode from the ideal trigonal-planar D_{3h} structure towards the T-shaped C_{2v} structure due to half-filled e' orbitals ($^1E'$ symmetry) (Scheme 1).[7, 8] The mexican-hat topology of this $E \otimes \varepsilon$ Jahn–Teller distortion then predicts that the Y-shaped structure is a first-order transition state for the permutation of the equatorial with the axial ligands.[9] The predicted T-shaped structure of $AuF_3(g)$ has recently been confirmed by gas-phase electron diffraction studies by Hargittai and co-

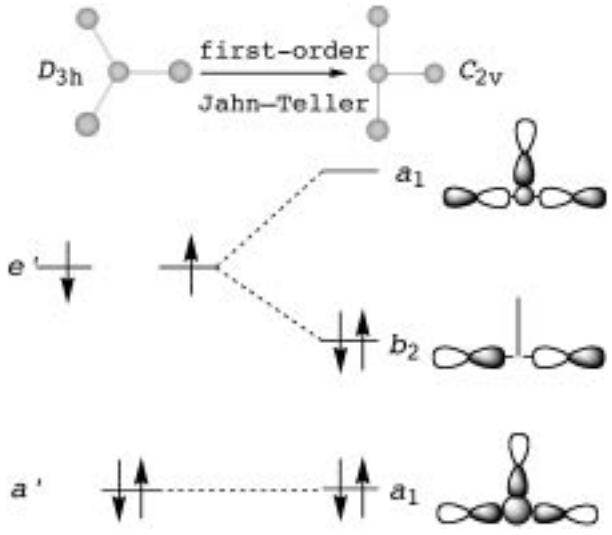

Scheme 1. Frontier orbitals for AuX_3 compounds with ligands X formally donating one p_σ electron each.

[a] Prof. Dr. P. Schwerdtfeger, Dr. T. Söhnel, R. Brown
Department of Chemistry, The University of Auckland
Private Bag 92019, Auckland (New Zealand)
Fax: (+64) 9-3737422
E-mail: schwerd@ccu1.auckland.ac.nz

[b] Prof. L. Kloo
Department of Chemistry, Inorganic Chemistry
Royal Institute of Technology
10044 Stockholm (Sweden)

  0947-6539/01/0714-3167 $ 17.50+.50/0

workers. Scheme 1 also shows that occupation of the a_1 LUMO instead of the b_2 HOMO leads to a favorable bonding interaction between the two equatorial ligands. There is no particular reason why the T-shaped AuX_3 structure should be the minimum and not the Y-shaped arrangement, especially for molecules where the lower oxidation state becomes more dominant, and the Y-shaped arrangement presents the path towards dissociation into AuX and X_2. In this case it will be difficult to obtain any gas-phase data for the monomer AuX_3. The predicted first-order Jahn–Teller distortion of AuX_3 compounds contrasts the finding by Choy et al. that AuI_3 adopts an ideal D_{3h} structure when intercalated in [Bi–O] layers of the $Bi_2Sr_2CaCu_2O_8$ superconductor.[10] This could imply a dynamic Jahn–Teller effect with rather low barriers between the T- and Y-shaped arrangements.

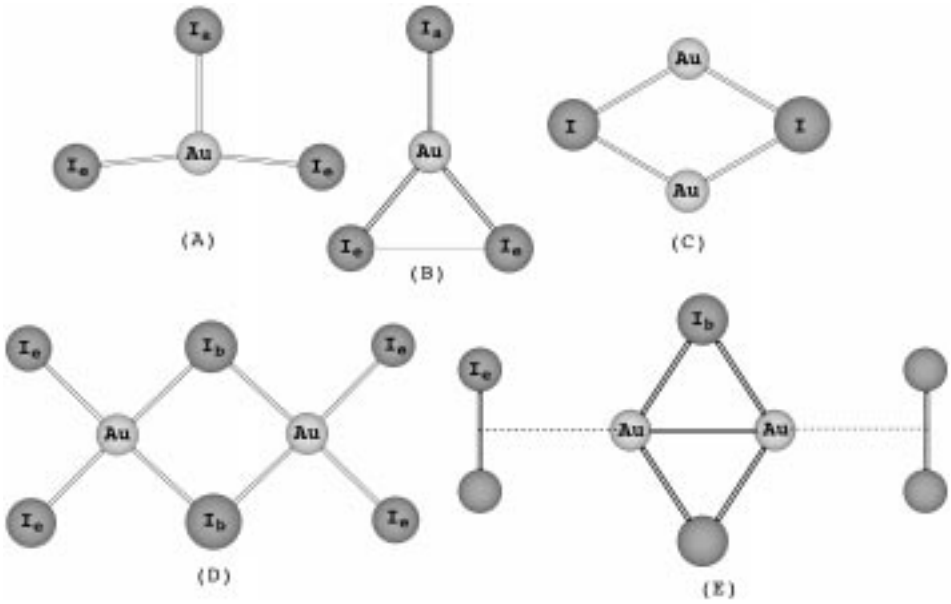

Figure 1. Optimized structures for A) T-shaped AuI_3, B) Y-shaped AuI_3, C) Au_2I_2, D) Au_2I_6, and E) I_2 molecules weakly interacting with Au_2I_2 at the RB3LYP level of theory.

Many of the unusual properties of gold compared to copper and silver are due to relativistic effects.[11, 12] Such effects are even more pronounced in superheavy elements such as eka-Au with nuclear charge 111.[13] It has been demonstrated in the past that the oxidation state +III of gold is relativistically stabilized.[14] AuI_4^- is the least stable of all halide compounds with a decomposition energy of about 30 kJ mol^{-1} for $AuI_4^- \rightarrow AuI_2^- + I_2$ at the MP4 (fourth order Møller–Plesset level) of theory.[7] In comparison this reduces to -70 kJ mol^{-1} at the nonrelativistic level. $AuBr_4^-$ is only slightly more stable than AuI_4^- (by 40 kJ mol^{-1} at the relativistic level)[7] and the question arises as to whether Au_2I_6 is a stable species similar to Au_2Br_6 and thus attempts should be made to isolate this compound.

To investigate the structure and stability of neutral gold(III) iodides we performed ab initio and density functional calculations for AuI, AuI_3, Au_2I_2, and Au_2I_6. We also considered AuI_3 trapped in between [Bi–O] layers of the $Bi_2Sr_2CaCu_2O_8$ superconductor in order to establish whether the AuI_3 unit is trigonal planar as suggested. To discuss possible decomposition products of AuI_3 we also investigated $(AuI)_2$ and finally solid-state $(AuI)_\infty$.

Computational Methods

The geometries of all compounds have been optimized at the second-order Møller-Plesset level (MP2) and B3LYP density functional (DFT) level using energy-adjusted small-core scalar relativistic and nonrelativistic pseudopotentials for Au and I.[11, 15] The structures are shown in Figure 1. The valence basis sets for Au used are as follows: (8s7p6d3f)/[7s4p5d3f] at the relativistic level (R) and (9s8p6d3f)/[8s7p5d3f] at the nonrelativistic level (NR). For iodine we used a (7s7p3d1f)/[6s6p3d1f] basis set at the relativistic and nonrelativistic levels.[11] For Au_2I_6 this resulted in 460 basis functions contracted to 406, which made MP2 and B3LYP geometry optimizations and frequency analyses very computer time extensive. For the coupled-cluster (singles–doubles with iterative triples, CCSD(T)) calculations of AuI we produced a potential energy curve of about 15 points. For this calculation we used more extensive valence basis sets for the (sp) part, that is a (11s9p8d3f)/[9s7p5d3f] basis set for gold and a (8s7p3d1f)/[7s7p2d1f] basis set for iodine. The spectroscopic parameters were derived by solving the vibrational–rotational Schrödinger equation numerically followed by a fit of the energy levels to a Dunham series.[16] For AuI_3 single-point CCSD(T) calculations at the optimized B3LYP geometries were carried out. The orbital space was kept fully active.

To simulate the [Bi–O] layers in $Bi_2Sr_2CaCu_2O_8$ we performed HF and LDA (local density approximation) calculations on finite Bi–O layers with the open valencies at the oxygen atoms saturated by H atoms using Hay–Wadt small-core pseudopotentials and smaller basis sets (LANL2MB). Two identical [Bi–O] layers were considered initially as shown in Figure 2: Model A with the two layers lying identically on top of each other as proposed by Choy et al,[10] and model B in which one layer is moved along the [Bi–O] plane such that the oxygens lie above the bismuth atoms and vice versa as observed in the X-ray structure of the superconductor.[17] For simplicity we assumed an idealized Bi–O distance of 2.705 Å within the layer.[17] Furthermore, we neglected modulation of the Bi atoms observed in the superconductor.[18] The SCF convergence of such a system was extremely slow and the geometry optimizations took several weeks on a multiprocessor SGI Origin 2000, which prohibited either MP2 or GGA density functional calculations or the inclusion of the next layer.

DFT B3LYP calculations for AuI and Au_2I_6 in the solid state were performed using the CRYSTAL98 program and the scalar relativistic

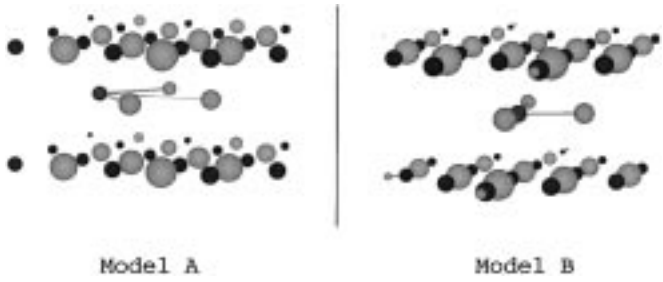

Figure 2. Optimized structure of AuI_3 intercalated in two different [Bi–O] layers (A) and (B). See text for details.

0947-6539/01/0714-3168 $ 17.50+.50/0 *Chem. Eur. J.* **2001**, *7*, No. 14

pseudopotentials as described above but with smaller basis sets.[19] For gold and iodine we used more compact (6s6p5d)/[4s3p3d] and (4s4p)/[3s3p] basis sets, respectively. The solid-state structure determined by Jagodzinski was used for AuI.[2] For Au_2I_6 we had to assume the structure obtained for solid Au_2Br_6[20] by scaling the size of the unit cell. The scaling factor of $\lambda \approx 1.10$ was determined by comparing the gas-phase structures of Au_2Br_6 with Au_2I_6.[21] The solid-state structures chosen are shown in Figure 3. We note that the ordering of the Au_2Br_6 units in the solid state is different from that of Au_2Cl_6. While the Au_2Br_6 molecules lie almost parallel to (001) the Au_2Cl_6 molecules are twisted alternatively to each other. It is assumed that (hypothetical) Au_2I_6 adopts rather the Au_2Br_6 crystal structure.

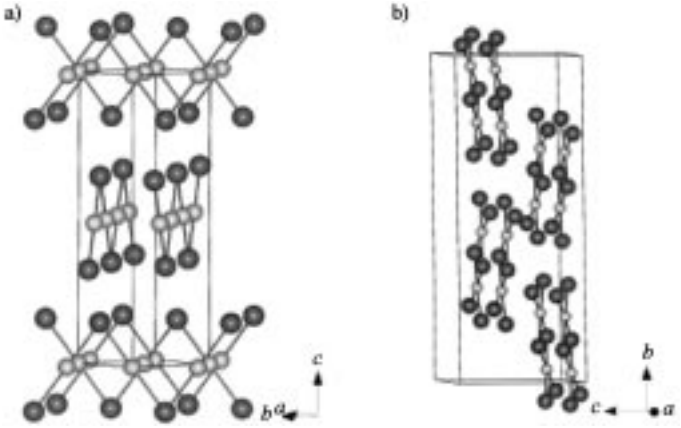

Figure 3. Solid-state structures for a) AuI and b) Au_2I_6 used in the calculations.

Results and Discussion

The optimized structures are shown in Figure 1. Bond lengths and angles are listed in Tables 1–3. Au_2I_6 has the predicted gas-phase structure with two iodine atoms bridging two gold atoms. Frequency analyses for AuI_3 show that the symmetric D_{3h} point represents a second-order saddle point, the E' distorted T-shaped structure a first-order saddle point, and the Y-shaped structure the minimum on the mexican-hat type Jahn–Teller potential energy surface (PES). The frequencies for the minimum structures are given in Table 4. We also investigated the linear Au-I-I-I structure which is a second-order saddle point; distortion to any bent structure optimizes either into the T-shaped or Y-shaped AuI_3 structure. An important result is that the Jahn–Teller topology is different to the one obtained for AuF_3 or $AuCl_3$, that is unlike the fluoride or the chloride the Y-shaped AuI_3 arrangement represents the minimum on the Jahn–Teller PES at both the MP2 and B3LYP level of theory. Single-point coupled-cluster (CCSD(T)) calculations on the B3LYP-optimized geometries confirm this, that is the Y-shaped structure is 7.6 kJ mol^{-1} lower in energy than the T-shaped structure, which is in very good agreement with the results from MP2 calculations. Additional geometry optimizations at the CCSD(T) level for AuI_3 do not change this result (Table 2), demonstrating that the B3LYP//CCSD(T) approach is a good approximation. The same topology is obtained at the nonrelativistic level. In fact, nonrelativistic AuI_3 is best described as I_2 weakly bound to AuI with a relatively large Au–I_e distance and a distance between the two equatorial iodine atoms of 2.69 Å close to the distance in free I_2 (2.658 Å). Indeed, Table 6 shows that the binding energy of I_2 to AuI is only 28 kJ mol^{-1} compared to 151 kJ mol^{-1} at the relativistic MP2 level. This again shows that the oxidation state +III in gold is relativistically stabilized.

The structures determined at the B3LYP and the MP2 levels agree within 0.1 Å and 1 degree. Table 5 gives CCSD(T) and MP2 results for AuI applying the larger basis set. A decrease of 0.026 Å in the Au–I bond length is calculated compared to the smaller basis set. The CCSD(T) bond length should be fairly accurate and we predict a Au–I distance of about 2.50 Å.

In all cases relativistic effects lead to a bond contraction as expected. The largest relativistic effect is observed for Y-shaped AuI_3 where the stabilization of the higher oxidation

Table 1. Optimized structural parameters for Au_2I_6 and Au_2I_2 at the relativistic (R) and nonrelativistic (NR) level of theory (MP2, B3LYP).[a]

Molecule	Method	r_b [Å]	r_e [Å]	r_{Au-Au} [Å]	∢(Au-Au-I_b) [°]	∢(Au-Au-I_e) [°]
Au_2I_6	RB3LYP	2.736	2.649	4.003	43.0	134.2
	RMP2	2.642	2.598	3.818	43.7	134.0
	NRB3LYP	2.847	2.739	4.166	43.0	136.6
	NRMP2	2.739	2.680	3.947	43.9	134.6
I_2-Au_2I_2-I_2	RB3LYP	2.795	3.677	2.803	59.9	158.4
	RMP2	2.729	3.159	2.634	61.1	154.7
	NRB3LYP	2.934	3.594	3.196	57.0	158.0
	NRMP2	2.861	3.319	3.005	58.3	156.2
Au_2I_2	RB3LYP	2.779	–	2.780	60.0	–
	RMP2	2.685	–	2.627	60.7	–
	NRB3LYP	2.917	–	3.092	58.0	–
	NRMP2	2.841	–	2.955	58.7	–

[a] For the notation of the iodine atoms see Figure 1. I_2-Au_2I_2-I_2 denotes Au_2I_6 with the equatorial iodine molecules weakly interacting with both Au atoms in Au_2I_2. Note that this structure is not a minimum on the potential hypersurface.

Table 2. Optimized structural parameters for AuI_3 and energy differences at the relativistic (R) and nonrelativistic (NR) level of theory (MP2, B3LYP).[a]

AuI_3	C_{2v} (T-shaped)			D_{3h}	C_{2v} (Y-shaped)				ΔE_1	ΔE_2
	r_a [Å]	r_e [Å]	∢(Au-I_a-I_e) [°]	r [Å]	r_a [Å]	r_e [Å]	$r(I_e - I_e)$ [Å]	∢(Au-I_a-I_e) [°]	[kJ mol^{-1}]	[kJ mol^{-1}]
RB3LYP	2.619	2.606	97.6	2.628	2.583	2.657	3.232	142.5	59.5	2.2
RMP2	2.561	2.548	96.2	2.570	2.522	2.570	3.245	140.8	76.0	8.5
RCCSD(T)	2.588	2.582	96.2	2.604	2.562	2.613	3.218	142.0	72.2	7.5
NRB3LYP	2.733	2.710	94.6	2.748	2.730	3.169	2.719	154.6	113.9	60.7
NRMP2	2.664	2.645	93.3	2.687	2.674	3.025	2.690	153.6	121.4	51.7

[a] For the notation of the iodine atoms see Figure 1. ΔE_1: Difference between the minimum Y-shaped structure and the D_{3h} second-order saddle point. ΔE_2: Difference between the Y-shaped structure and the T-shaped first-order saddle point.

Table 3. Optimized bond lengths for AuI and I_2.

	r_e(Au–I) [Å]	r_e(I_2) [Å]
Exp.[a]	–	2.666
RB3LYP	2.552	2.704
RMP2	2.486	2.678
NRB3LYP	2.726	2.683
NRMP2	2.675	2.658

[a] Experimental value from reference [30].

Table 5. Spectroscopic properties for AuI.[a]

AuI	RCCSD(T)	RMP2	RB3LYP
bond length r_e [Å]	2.506	2.460	2.538
dissociation energy D_0 [kJ mol^{-1}]	200.9	202.4	186.4
vibrational frequency ω_e [cm^{-1}]	209	226	194
anharmonic vibration constant $\omega_e x_e$ [cm^{-1}]	0.470	0.404	0.399
rotational constant B_e [10^{-2} cm^{-1}]	3.477	3.610	3.389
vibration–rotation coupling constant α_e [10^{-5} cm^{-1}]	9.36	9.17	9.70
centrifugal distortion constant D_e [10^{-9} cm^{-1}]	3.87	3.65	4.10

[a] D_0 corrected for zero-point vibrational energy and atomic spin-orbit contribution.[32] The atomic masses (in amu) of 196.9666 for Au and 126.9004 for iodine were used.

state leads to a shortening of the Au–I_e bond of about 0.5 Å which can be described by a change in the oxidation state from +1 to +3. We also note that the Au–Au distance in Au_2I_6 decreases by about 0.2 Å due to relativistic effects. However, this is not due to aurophilic interactions but is rather well described by the Au–I_b relativistic bond contraction. This is supported by the fact that the relativistic change in the Au-Au-I_b bond angle is insignificant. In contrast, Au_2I_2 shows a very small Au–Au distance of 2.78 Å and a relativistic change in the Au-Au-I_b bond angle of 2°. In this case we cannot fully exclude aurophilic interactions.

A comparison between previously calculated bond angles for T-shaped structures of AuF_3 and $AuCl_3$ (93° for both)[8] shows that for AuI_3 (96° at the MP2 level, Table 2) this angle is larger than expected resulting probably from the steric hindrance of the larger iodine atoms. For AuI_3 the axial Au–I bond length is larger than the equatorial distance for the T-shaped structure and vice versa for the Y-shaped arrangement. This is true at both the relativistic and nonrelativistic level of theory. In contrast, for AuF_3 and $AuCl_3$ at the relativistic level the axial Au–X bond length is smaller than the equatorial one.

The Jahn–Teller $D_{3h} \rightarrow C_{2v}$ stabilization is rather large, 76 kJ mol^{-1} at the RMP2 and 60 kJ mol^{-1} at the RB3LYP level. It is therefore more than questionable whether AuI_3 can adopt an ideal D_{3h} trigonal-planar structure when intercalated in [Bi–O] layers in the $Bi_2Sr_2CaCu_2O_8$ superconductor which crystallizes tetragonally, in the idealized case.[17] With this, the environment between two [Bi–O] layers in the $Bi_2Sr_2CaCu_2O_8$ superconductor does not contain local C_3 symmetry. The quasi-tetragonal structure of the superconductor should be an ideal matrix for the T-shaped AuI_3. Indeed, model calculations simulating such an environment (see Figure 2) do not preserve the starting geometry of D_{3h} symmetry.

In the case of model A AuI_3 dissociates with the gold atom linked to two Bi atoms in the top and bottom layers. This can easily be explained. First the interlayer distance between the Bi atoms is 6.27 Å (compared to 6.89 Å for model B layer) and large enough for accommodating even larger atoms like Au or I. Second, gold is well known to form very strong intermetallic bonds due to relativistic effects.[22] Next, it is clear that iodine is rather bound to Bi than oxygen. The Au–I distance is 3.97 Å and comparable to the intralayer Bi–Bi distance of 3.83 Å. This arrangement does not agree at all with the results of Choy et al.[10] and indicates that model B may be a better candidate for the intercalated superconductor.

Turning now to model B, AuI_3 adopts a T-shaped structure as we would expect from local symmetry. The gold and iodine atoms occupy interlayer [Bi–O] sites which again supports a T-shaped structure. The Bi–O bond length of 2.71 Å is also not too different from the Au–I distance (2.51 Å) given by Choy et al.[10] However, the optimized Au–I bond lengths at the LDA level are 3.13 Å for the equatorial bond and 3.41 Å for the axial bond, which are far too long. This is probably due to the small basis sets used and the neglect of additional layers in the superconductor leading to weaker Au–I bonding. Indeed, HF (LDA) optimizations of free AuI_3 with the LANL2MB version of the Hay–Wadt basis sets leads to bond lengths for the T-shaped structure of $r_a = 2.879$ Å and $r_e = 2.787$ Å ($r_a = 2.830$ Å and $r_e = 2.742$ Å) which are too long, and to I_a-Au-I_e bond angles of 91.8° (96.3°). An interesting feature is that the gold atom is more closely bound to the Bi atom on one layer which causes a distortion away from local C_{2v} symmetry in AuI_3. Anyway, the calculations support a local (slightly distorted) T-shaped structure for AuI_3 and not a

Table 4. Vibrational frequencies for various gold iodides.[a]

Molecule	Method	Frequencies [cm^{-1}]
Au_2I_6	RB3LYP	A_g: 44, 74, 138, 187; A_u 21; B_{1g} 39, 64; B_{1u} 61 s, 130 m, 184 vs; B_{2u} 15 m, 73; B_{2g}, 60, 187; B_{3u} 33 m, 125, 193 s; B_{3g} 118
AuI_3	RB3LYP	A_1 45 s, 150, 205 vs; B_1 53; B_2 25, 151
	RMP2	A_1 78 s, 179, 243 vs; B_1 59; B_2 18, 195
Au_2I_2	RB3LYP	A_g 77, 154; B_{1u} 138 vs; B_{2u} 41; B_{2g} 75; B_{3u} 65 s
	RMP2	A_g 112, 193; B_{1u} 170 vs; B_{2u} 43; B_{2g} 99; B_{3u} 77 s
AuI	RB3LYP	192
	RMP2	226
I_2	RB3LYP	213
	RMP2	229

[a] The IR intensities are classified as follows: very strong (vs), strong (s), or medium (m). All other frequencies are either weak or absent in the IR spectrum. The definition according to Nakamoto[31] for the symmetry assignments is used (for Au_2I_6 and Au_2I_2 the molecules lie in the xz plane).

0947-6539/01/0714-3170 $ 17.50+.50/0 *Chem. Eur. J.* **2001**, *7*, No. 14

D_{3h} trigonal-planar structure as suggested. However, if the AuI_3 distortion is dynamic in nature it may be difficult to observe this Jahn–Teller effect.

Table 6 shows a thermochemical analysis for the individual decomposition reactions for the gold iodides. For the total decomposition $Au_2I_6 \rightarrow Au_2I_2 + 2\,I_2$ we obtain $\Delta H^0 = 141\ kJ\,mol^{-1}$ and $\Delta G^0 = 54\ kJ\,mol^{-1}$ at the relativistic B3LYP level. This shows that Au_2I_6 is reasonably stable and it may be possible (albeit difficult) to detect this in matrix isolation. We note that the MP2 values are probably overestimated. In a recent paper we showed that the MP2 series considerably overestimates decomposition for high oxidation state fluorides, and that the result obtained at the B3LYP level is in good agreement with more accurate coupled-cluster results.[23] To demonstrate that this is the case for the gold iodides as well we carried out a single-point CCSD(T) calculation for Y-shaped AuI_3 at the RB3LYP geometry. Using optimized CCSD(T) geometries for the decomposition products AuI and I_2 we obtain a CCSD(T) value of $97.3\ kJ\,mol^{-1}$ for $AuI_3 \rightarrow AuI + I_2$ which is larger than the B3LYP value of $61.2\ kJ\,mol^{-1}$ but much lower than the MP2 value of $150.6\ kJ\,mol^{-1}$ (Table 6). The ΔG^0 value given above may therefore be underestimated by about $30-40\ kJ\,mol^{-1}$.

Table 6. Thermochemical gas phase data for the decomposition of Au_2I_6, AuI_3, and Au_2I_2.[a]

ΔE [kJ mol^{-1}] RB3LYP	ΔE [kJ mol^{-1}] RMP2	ΔE [kJ mol^{-1}] NRB3LYP	ΔE [kJ mol^{-1}] NRMP2	ΔG^0 [kJ mol^{-1}] RB3LYP	ΔH^0 [kJ mol^{-1}] RB3LYP	ΔS^0 [J mol^{-1}K^{-1}] RB3LYP
$Au_2I_6 \rightarrow 2\,AuI_3$						
153.4	266.5	23.2	133.1	77.3	135.3	194.5
$2\,AuI_3 \rightarrow 2\,AuI + 2\,I_2$						
122.4	301.2	30.1	56.3	50.4	117.3	224.1
$Au_2I_2 \rightarrow 2\,AuI$						
114.5	220.5	148.1	198.1	73.5	112.1	129.6

[a] All energies in kJ mol^{-1} at 298.15 K and 1 atm. ΔE: difference in total electronic energies (without zero-point vibrational correction). For AuI_3 the Y-shaped minimum is taken. For the reaction $2\,AuI_3 \rightarrow 2\,AuI + 2\,I_2$ thermodynamic parameters at the RMP2 level were calculated as well (in kJ mol^{-1}): $\Delta G^0 = 225.8$, $\Delta H^0 = 295.4$, $\Delta S^0 = 333.4$.

To discuss the stability of Au_2I_6 in the solid state one has to know the cohesive or lattice energies of the respective crystals. However, only the crystal structure of AuI is known. Solid-state calculations using the measured crystal structure (Au–I distance of 2.604 Å) and the same bond length for free AuI gives a sublimation energy of $\Delta E_{sub} = 158.1\ kJ\,mol^{-1}$ for $AuI(s) \rightarrow AuI(g)$ at the relativistic B3LYP level. This is much higher than the dimerization energy of AuI which is only $57.3\ kJ\,mol^{-1}$ (Table 6). Nevertheless, the change in total energy (neglecting thermal effects) for the process $Au_2I_6(g) \rightarrow 2AuI(s) + 2\,I_2(g)$ is still positive ($58.9\ kJ\,mol^{-1}$). If we optimize the structure for AuI(g) we obtain 2.566 Å which lowers the sublimation energy by only $1.0\ kJ\,mol^{-1}$. More significant is the structural change in solid AuI when optimized at the B3LYP level leading to a Au–I bond length of 2.684 Å. However, the sublimimation energy again changes little, $\Delta E_{sub} = 162.7\ kJ\,mol^{-1}$. The sublimation energy of Au_2I_6 for the process $Au_2I_6(s) \rightarrow Au_2I_6(g)$ is expected to be small and will further increase the energy necessary for the decomposition of Au_2I_6. An attempt to calculate the sublimation energy using the RB3LYP structure of Au_2I_6 with estimated lattice parameters gave only a small positive value. This is easily understood since we only expect weak interactions between Au_2I_6 units and DFT is currently not able to describe such situations accurately. Moreover, a complete geometry optimization for the solid state is needed to get accurate sublimation energies. A single-point solid-state B3LYP calculation required about 1 day on a supercomputer and a geometry optimization is therefore not feasible. Nevertheless, according to our calculations the synthesis of Au_2I_6 should be attempted. Our finding is also supported by empirical estimates of the enthalpy of formation ΔH_f for a series of unknown metal halides published by Hisham and Benson.[24] They report a ΔH_f value between -5 and $-15\ kJ\,mol^{-1}$ for AuI_3.

To discuss whether the Au_2I_6 structure shown in Figure 1 is the global minimum on the potential hypersurface we also considered the case of two I_2 molecules weakly interacting with Au_2I_2 as shown in Figure 1E. The structural parameters listed in Table 1 show what is expected for such a structure. The distances and angles in the Au_2I_2 unit of I_2-Au_2I_2-I_2 resemble closely the one for free Au_2I_2. The weak interactions with the I_2 molecules increase the Au–Au bond length and thus diminish aurophilic interactions. The distance from one gold atom to the center of the iodine molecule is 3.216 Å at the relativistic level and 3.332 Å at the nonrelativistic level. The most interesting fact however is that for nonrelativistic Au_2I_6 the weak I_2-Au_2I_2-I_2 complex is more stable by $82.2\ kJ\,mol^{-1}$, whilst at the relativistic level it is less stable by $142.5\ kJ\,mol^{-1}$ than structure D in Figure 1 at the B3LYP level of theory. This again demonstrates the change in oxidation state from +I to +III by relativistic effects. We note that the I_2 interaction with Au_2I_2 is indeed weak, only 23.2 (12.6) $kJ\,mol^{-1}$ at the relativistic (nonrelativistic) B3LYP level and 87.1 (69.7) $kJ\,mol^{-1}$ at the relativistic (nonrelativistic) MP2 level. This is also reflected in the I–I bond length of the terminal I_2 subunit, which is 2.710 (2.701) Å at the relativistic B3LYP (MP2) level and 2.693 (2.674) Å at the nonrelativistic level, and therefore close to the one calculated for free I_2. As expected, the Au–I bond length of I_2 weakly interacting with the gold atom is very sensitive to the method applied (Table 1). We note that the optimized relativistic I_2-Au_2I_2-I_2 structure is not a minimum on the potential energy surface but a higher order saddle point with modes describing the rotation of the I_2 molecules out of the Au_2I_2 plane and distortions from D_{2h} symmetry. Since these are energetically only small distortions we did not investigate this further.

Using the calculated CCSD(T) gas phase dissociation energy of AuI ($200.9\ kJ\,mol^{-1}$) we obtain a cohesive energy of $\Delta E_{coh} = \Delta E_{sub} + D_0(AuI) = 359\ kJ\,mol^{-1}$, which is about $160\ kJ\,mol^{-1}$ smaller than that for AuCl ($\Delta E_{coh} =$

522.2 kJ mol^{-1}).[25] On the other hand if we take the dissociation energy of AuCl (275 kJ mol^{-1})[26] we obtain $\Delta E_{sub} =$ 247 kJ mol^{-1} for AuCl, which is 90 kJ mol^{-1} higher than that for AuI. This agrees with the fact that AuI decomposes before melting at about 120 °C and AuCl decomposes around 170 °C. We note that recent solid-state calculations for AuCl by Doll et al. showed that correlation effects are important for the accurate determination of structures and cohesive energies.[27]

The lattice energies ΔE_{lat} of AuX (X = Cl, Br and I) have been estimated, and interestingly, they are all around 1015 kJ mol^{-1}.[28] This suggests that the differences in cohesive energy is dominated by the differences in the electron affinity of the halide ligand (in kJ mol^{-1}: Cl 348, Br 324, I 296).[29] However, this only explains 1/3 of the difference between AuCl and AuI. If we take the first ionization potential of gold (890.1 kJ mol^{-1}) and the electron affinity of iodine we obtain $\Delta E_{coh} = 421$ kJ mol^{-1}, which is in reasonable agreement with our calculated B3LYP value. Differences are due to the approximation applied and to experimental inaccuracies in the lattice energy.

Conclusion

We have investigated the structure and stability of a number of gold +I and +III iodides in the gas phase and the solid state. The major conclusions are:

- For diatomic AuI spectroscopic properties are predicted which should help to identify this molecule in matrix isolation. The cohesive energy of 359 kJ mol^{-1} calculated at the B3LYP level of theory is in reasonable agreement with the experimental value (421 kJ mol^{-1}).
- Au_2I_6 is thermodynamically stable both in the gas phase and in the solid state and it should be possible to isolate this compound despite unsuccessful attempts more than thirty years ago.[33]
- AuI_3 is Jahn–Teller distorted as expected, but the Y-shaped structure is the minimum. For AuI_3 intercalated in [Bi–O] layers of cuprite superconductors a T-shaped structure is predicted according to the local tetragonal environment.
- Nonrelativistic AuI_3 is best described by I_2 weakly bound to AuI. Similarly, Au_2I_6 at the nonrelativistic level can be best described as two I_2 molecules weakly bound to Au_2I_6. Hence the change in oxidation state from +I to +III of Au is due to relativistic effects.
- The calculations on AuI show that MP2 leads to bond lengths that are too short compared to those obtained with the more accurate CCSD(T) procedure. B3LYP tends to give bond lengths that are slightly overestimated. Both methods, however, lead to reasonable estimates for energy differences. For the higher oxidation state this is not the case anymore. MP2 overbinds, whilst B3LYP probably underestimates decomposition energies. Difficulties with decomposition energies of transition metal compounds in higher oxidation states have been reported before.[23]

Acknowledgement

This work was supported by Alexander von Humboldt Foundation (Bonn, Germany), the Marsden Fund (Wellington), and the Auckland University Research Committee. We thank Prof. R. Hoffmann, M. Munzarova (Cornell), and M. Hargittai (Budapest) for interesting discussions.

[1] a) R. J. Puddephatt in *Comprehensive Coordination Chemistry*, *Vol.5*, Pergamon, Oxford, England, **1987**, p 861; b) M. Melnik, R. V. Parish, *Coord. Chem. Rev.* **1986**, *70*, 157; c) M. C. Gimeno, A. Laguna, *Chem. Rev.* **1997**, *97*, 511.
[2] H. Jagodzinski, *Z. Kristallogr.* **1959**, *112*, 80.
[3] a) C. J. Evans, M. C. L. Gerry, *J. Am. Chem. Soc.* **2000**, *122*, 1560; b) C. J. Evans, M. C. L. Gerry, *J. Mol. Spect.* **2000**, *203*, 105.
[4] J. L. Ryan, *Inorg. Chem.* **1969**, *8*, 2058.
[5] J. Strähle, J. Gelinek, M. Kolmel, A. M. Nemecek, *Z. Naturforsch. B* **1979**, *34*, 952.
[6] A. Hakansson, L. Johansson, *Chem. Scr.* **1975**, *7*, 201.
[7] P. Schwerdtfeger, P. D. W. Boyd, S. Brienne, A. K. Burrell, *Inorg. Chem.* **1992**, *31*, 3411.
[8] P. Schwerdtfeger, H. Schmidbaur, *Z. Anorg. Allg. Chem.* **2000**, *626*, 374.
[9] P. Schwerdtfeger, P. Hunt in *Adv. Mol. Struct. Res.*, *Vol. 5* (Eds.: M. Hargittai, I. Hargittai), JAI Press Inc., Stanford, USA, **1999**, pp. 223–262.
[10] J.-H. Choy, Y.-I. Kim, S.-J. Hwang, P. V. Huong, *J. Phys. Chem. B* **2000**, *104*, 7273.
[11] a) P. Schwerdtfeger, M. Dolg, W. H. E. Schwarz, G. A. Bowmaker, P. D. W. Boyd, *J. Chem. Phys.* **1989**, *91*, 1762; b) P. Schwerdtfeger, P. D. W. Boyd, *Inorg. Chem.* **1992**, *31*, 327; c) P. Schwerdtfeger, G. A. Bowmaker, *J. Chem. Phys.* **1994**, *100*, 4487.
[12] a) P. Pyykkö, *Chem. Rev.* **1988**, *88*, 563; b) W. H. E. Schwarz, "Fundamentals of Relativistic Effects in Chemistry" in *Theoretical Models of Chemical Bonding, Vol. II* (Ed.: Z. B. Maksic), Springer, Heidelberg, **1989**, p. 593.
[13] P. Schwerdtfeger, M. Seth in *Encyclopedia of Computational Chemistry*, *Vol. 4* (Eds.: P. von R. Schleyer, P. R. Schreiner, N. L. Allinger, T. Clark, J. Gasteiger, P. A. Kollman, H. F. Schaefer III), Wiley, New York, **1998**, pp. 2480–2499.
[14] P. Schwerdtfeger, *J. Am. Chem. Soc.* **1989**, *111*, 7261.
[15] M. J. Frisch, G. W. Trucks, H. B. Schlegel, G. E. Scuseria, M. A. Robb, J. R. Cheeseman, V. G. Zakrzewski, J. A. Montgomery, Jr., R. E. Stratmann, J. C. Burant, S. Dapprich, J. M. Millam, A. D. Daniels, K. N. Kudin, M. C. Strain, O. Farkas, J. Tomasi, V. Barone, M. Cossi, R. Cammi, B. Mennucci, C. Pomelli, C. Adamo, S. Clifford, J. Ochterski, G. A. Petersson, P. Y. Ayala, Q. Cui, K. Morokuma, D. K. Malick, A. D. Rabuck, K. Raghavachari, J. B. Foresman, J. Cioslowski, J. V. Ortiz, B. B. Stefanov, G. Liu,A. Liashenko, P. Piskorz, I. Komaromi, R. Gomperts, R. L. Martin, D. J. Fox, T. Keith, M. A. Al-Laham, C. Y. Peng, A. Nanayakkara, C. Gonzalez, M. Challacombe, P. M. W. Gill, B. Johnson, W. Chen, M. W. Wong, J. L. Andres, C. Gonzalez, M. Head-Gordon, E. S. Replogle, J. A. Pople, Gaussian 98, Gaussian, Inc., Pittsburgh, PA, **1999**.
[16] a) S. Wilson in *Methods in Computational Chemistry*, *Vol. 4* (Ed.: S. Wilson), Plenum, New York, **1992**, 1; b) K. Andersson, M. R. A. Blomberg, M. P. Fülscher, V. Kellö, R. Lindh, P.-Aa. Malmqvist, J. Noga, J. Olsen, B. O. Roos, A. J. Sadlej, P. E. M. Siegbahn, M. Urban, P.-O. Widmark, MOLCAS, Version 2, University of Lund, Sweden, **1991**; c) J. L. Dunham, *Phys. Rev.* **1932**, *41*, 721.
[17] J. K. Liang, S. S. Xie, G. C. Che, J. Q. Huang, Y. L. Zhang, Z. X. Zhao, *Mod. Phys. Lett.* **1988**, *2*, 483.
[18] M. Hervieu, C. Michel, B. Domenges, Y. Laligant, A. Lebail, G. Ferey, B. Raveau, *Mod. Phys. Lett.* **1988**, *2*, 491.
[19] V. R. Saunders, R. Dovesi, C. Roetti, M. Causà, N. H. Harrison, R. Orlando, C. M. Zicovich-Wilson, Program CRYSTAL98, University of Torino, Torino, **1998**.
[20] K. P. Lörchner, Y. Strähle, *Z. Naturforsch. B* **1975**, *30*, 662.
[21] E. S. Clark, D. H. Templeton, C. H. MacGillavry, *Acta Crystallogr.* **1958**, *11*, 284.
[22] P. Schwerdtfeger, M. Dolg, *Phys. Rev. A* **1991**, *43*, 1644.
[23] M. Seth, F. Cooke, M. Pelissier, J-L. Heully, P. Schwerdtfeger, *J. Chem. Phys.* **1998**, *109*, 3935.
[24] a) M. W. M. Hisham, S. W. Benson, J. *Chem. Eng. Data* **1992**, *37*, 194; b) M. W. M. Hisham, S. W. Benson,*J. Phys. Chem.* **1987**, *91*, 3631.
[25] *CRC Handbook of Chemistry and Physics*, 75th ed. (Ed.: D. R. Lide), CRC Press, Boca Raton, Florida, **1994**.
[26] P. Schwerdtfeger, *Mol. Phys.* **1995**, *86*, 359.
[27] K. Doll, P. Pyykkö, H. Stoll, *J. Chem. Phys.* **1998**, *109*, 2339.
[28] D. D. Wagman, W. H. Evans, V. B. Parker, R. H. Churney, R. L. Nuttall, *J. Phys. Chem. Ref. Data (Suppl. 2)* **1982**, *11*.

  0947-6539/01/0714-3172 $ 17.50+.50/0

[29] H. Hotop, W. C. Lineberger, *J. Phys. Chem. Ref. Data* **1985**, *14*, 731.
[30] K. P. Huber, G. Herzberg, *Molecular Spectra and Molecular Structure, Constants of Diatomic Molecules*, Van Nostrand, New York, **1979**.
[31] K. Nakamoto, *Infrared and Raman Spectra of Inorganic and Coordination Compounds*, Wiley, New York, **1997**.
[32] C. E. Moore, *Atomic Energy Levels*, NSRDS-NBS 35/*Vol. I-III*, Nat. Bur. Standards, Washington, DC, **1958**.
[33] M. O. Faltensand, D. A. Shirley, *J. Chem. Phys.* **1970**, *53*, 4249.

Received: January 26, 2001 [F3026]

  0947-6539/01/0714-3173 $ 17.50+.50/0